Vol. 36 (2005) ACTA PHYSICA POLONICA B No 6

COMPARISON OF TWO STATIONARY SPHERICAL ACCRETION MODELS

Bogusz Kinasiewicz

The M. Smoluchowski Institute of Physics, Jagellonian University
Reymonta 4, 30-059 Kraków, Poland

Tomasz Lanczewski

The H. Niewodniczański Institute of Nuclear Physics PAN
Radzikowskiego 152, 31-342 Kraków, Poland

(Received February 8, 2005)

The general relativistic gas accretion onto a black hole is investigated in which the flow is steady and spherically symmetrical. Two models with different equations of state are compared. Numerical calculations show that the predictions of the models are similar in most aspects. In the ultrarelativistic regime the allowed band of the speed of sound and the mass accretion rate can be markedly different.

PACS numbers: 04.70.Bw

1. Introduction

The accretion of gas on compact objects (white dwarfs, neutron stars, black holes) has not been entirely investigated by now, even in the simplest case of spherically symmetrical systems. The study of accretion has its beginnings in the paper presented by Bondi [1]. He considered spherically symetrical accretion on the basis of Newtonian gravity. Further progress has been made by Michel [2] and Shapiro and Teukolsky [3] who gave a general relativistic version of the Bondi model — the $(\tilde{p} - n)$ model — as we call it latter on. Another relativistic generalization was given by Malec [4] — the $(\tilde{p} - \varrho)$ model — in what follows.

It is not clear which equation of state is appropriate in the description of relativistic collapsing gas. There are two commonly used polytropic equations of state: $\tilde{p} = K\varrho^{\Gamma}$ [3] and $\tilde{p} = Cn^{\Gamma}$ [4]. Here $\tilde{p}$ is the pressure, ϱ the energy density and n the baryonic mass density. The intention of this paper is to compare predictions of both models concerning the sound velocity, the fluid velocity, the density and the mass accretion rate. Here the $(\tilde{p} - \varrho)$ model and the $(\tilde{p} - n)$ model denotes the model with the equation of state given by $\tilde{p} = K\varrho^{\Gamma}$ and $\tilde{p} = Cn^{\Gamma}$, respectively.

The order of this work is as follows. In Section 2 we briefly present $(\tilde{p}-n)$ and $(\tilde{p} - \varrho)$ models. Section 3 is dedicated to the comparison of predictions of both models using the results of numerical calculations. In the course of the paper we set $G = c = 1$ everywhere.

2. The spherical accretion onto a black hole

Let us consider a spherically symmetric cloud of an ideal gas falling onto a Schwarzschild black hole. The most suitable choice of the system of coordinates for the description of self-gravitating matter is the comoving frame — the so called Lagrangian approach. The general spherically symmetric line element is given by

$$ds^2 = -N^2 dt^2 + \alpha dr^2 + R^2 d\theta^2 + R^2 \sin^2\theta d\phi^2\,, \tag{1}$$

where N, α and R depend on the asymptotic time variable t and the radius r.

The energy-momentum tensor of evolving perfect fluid can be written in the form

$$T_{\mu\nu} = (\varrho + \tilde{p})u_\mu u_\nu + \tilde{p}g_{\mu\nu}\,, \tag{2}$$

where u_μ is the four-velocity of the fluid, $\tilde{p}$ the pressure and ϱ denotes the energy density.

The form of the flow is governed by two fundamental equations: the continuity equation

$$R^2\partial_t\varrho = -N(\varrho + \tilde{p})\partial_R(UR^2) \tag{3}$$

and the relativistic Euler equation

$$N\partial_R\tilde{p} + (\tilde{p} + \varrho)\partial_R N = 0\,. \tag{4}$$

It should be emphasized that Eqs. (3), (4) and the equation of state describe the fluid accretion in a fixed space-time (Schwarzschild) geometry. The motion of the gas is assumed to be adiabatic which means that the index Γ is constant and belongs to the interval $1 < \Gamma \leq \frac{5}{3}$.

In our paper we neglect the effect of backreaction that is the change of geometry caused by infalling gas is regarded to be negligible. Then one finds [4] that

$$N \approx \sqrt{1 - \frac{2M}{R} + U^2}\,.$$

It is useful to introduce the sound velocity as follows

$$a^2 = \frac{d\tilde{p}}{d\varrho}\,.$$

The accreting flow may be subsonic or supersonic and there exists a characteristic point (the so-called sonic point $R = R_\mathrm{s}$) at which the infall velocity and the speed of sound satisfy

$$|U| = Na.$$

2.1. The $(\tilde{p} - \varrho)$ model of stationary accretion

The $(\tilde{p} - \varrho)$ model is based on the assumption that the gas respects the polytropic equation of state in terms of the energy density ϱ:

$$\tilde{p} = K\varrho^{\Gamma},$$

where the constant K is totally dependent on boundary conditions $K = p_\infty/\varrho_\infty^{\Gamma}$. The integrated equation (4) can be also expressed in terms of the sound velocity

$$a^2 = -\Gamma + \frac{\Gamma + a_\infty^2}{N^\kappa}, \tag{5}$$

where $\kappa = (\Gamma - 1)/\Gamma$ and the integration constant a_∞^2 is equal to the asymptotic velocity of sound at the outer boundary of the cloud.

The sound velocity is given by

$$a^2 = K\Gamma\varrho^{\Gamma-1}.$$

One may analyse (5) at the sonic point to get:

$$\left(\frac{a_\infty^2 + \Gamma}{a_\mathrm{s}^2 + \Gamma}\right)^{2/\kappa} (1 + 3a_\mathrm{s}^2) = 1\,. \tag{6}$$

Further on we omit details that can be found in [4] and write down the final equations.

The fluid velocity is found to be [4]

$$U^2 = \frac{R_\mathrm{s}^3 M}{2R^4}\left(\frac{1}{1 + \Gamma/a_\mathrm{s}^2}\right)^{2/(\Gamma-1)} \left(1 + \frac{\Gamma}{a^2}\right)^{2/(\Gamma-1)}. \tag{7}$$

Now, from the relation between pressure and energy density one obtains that

$$\varrho = \varrho_\infty\left(\frac{a}{a_\infty}\right)^{2/(\Gamma-1)} = \varrho_\infty\left(-\frac{\Gamma}{a_\infty^2} + \frac{\Gamma/a_\infty^2 + 1}{N^\kappa}\right)^{1/(\Gamma-1)}, \tag{8}$$

where the constant ϱ_∞ is the asymptotic mass density of the collapsing fluid. The mass accretion rate can be described by means of the formula [4]:

$$\dot{M} = \pi M^2 \frac{\varrho_\infty}{a_\infty^3} \left(\frac{a_{\rm s}^2}{a_\infty^2}\right)^{(5-3\Gamma)/2(\Gamma-1)} \left(1 + \frac{a_{\rm s}^2}{\Gamma}\right) \left(1 + 3a_{\rm s}^2\right). \tag{9}$$

2.2. The ($\tilde{p} - n$) model of stationary accretion

In this section we briefly present the ($\tilde{p} - n$) model (for detailed description see [2, 3] or [7]).

It is an often practice that astrophysicists express the equation of state in terms of baryonic density:

$$\tilde{p} = Cn^\Gamma,$$

where the constant $C = p_\infty / n_\infty^\Gamma$.

In place of equation (4) one can again use the Bernoulli equation

$$\Gamma - 1 - a^2 = N\left(\Gamma - 1 - a_\infty^2\right). \tag{10}$$

Here the square of the sound velocity is given by

$$a^2 = \frac{C\Gamma n^{\Gamma-1}}{1 + \frac{C\Gamma}{\Gamma-1} n^{\Gamma-1}}.$$

One may easily notice that $a^2 < \Gamma - 1$ (see also [3]). Let us point out that there is no such restriction in the ($\tilde{p} - \varrho$) model.

Evaluation of the Bernoulli equation at the sonic point yields

$$\left(1 + 3a_{\rm s}^2\right)\left(1 - \frac{a_{\rm s}^2}{\Gamma - 1}\right)^2 = \left(1 - \frac{a_\infty^2}{\Gamma - 1}\right)^2. \tag{11}$$

The fluid velocity reads

$$U = \frac{1}{4R^2}\left(\frac{a_{\rm s}^2}{a^2}\sqrt{1 - \frac{2M}{R} + U^2}\right)^{1/(\Gamma-1)} \left(\frac{1 + 3a_{\rm s}^2}{a_{\rm s}^2}\right)^{3/2}, \tag{12}$$

where the baryonic density can be expressed in terms of a^2 as follows:

$$n = n_\infty \left[\frac{a^2}{a_\infty^2}\left(\frac{\Gamma - 1 - a_\infty^2}{\Gamma - 1 - a^2}\right)\right]^{1/(\Gamma-1)}. \tag{13}$$

One can determine the mass accretion rate by [3]

$$\dot{M} = \pi M^2 n_\infty \left(\frac{a_{\rm s}^2}{a_\infty^2} \cdot \sqrt{1 + 3a_{\rm s}^2}\right)^{1/(\Gamma-1)} \left(\frac{1 + 3a_{\rm s}^2}{a_{\rm s}^2}\right)^{3/2}. \tag{14}$$

3. Numerical calculations

In this section we compare both models numerically referring to certain parameters important for the description of the process of accretion (see also [5]).

3.1. Evaluation of parameter a_s^2

First we analyse the solutions of Eq. (11) for certain values of Γ and compare them to the solutions of Eq. (6) in the $(\tilde{p}-\varrho)$ model. Our calculations are shown in Fig. 1. As one can see, in the $(\tilde{p}-n)$ model the greater Γ the greater value of a_s^2 is reached.

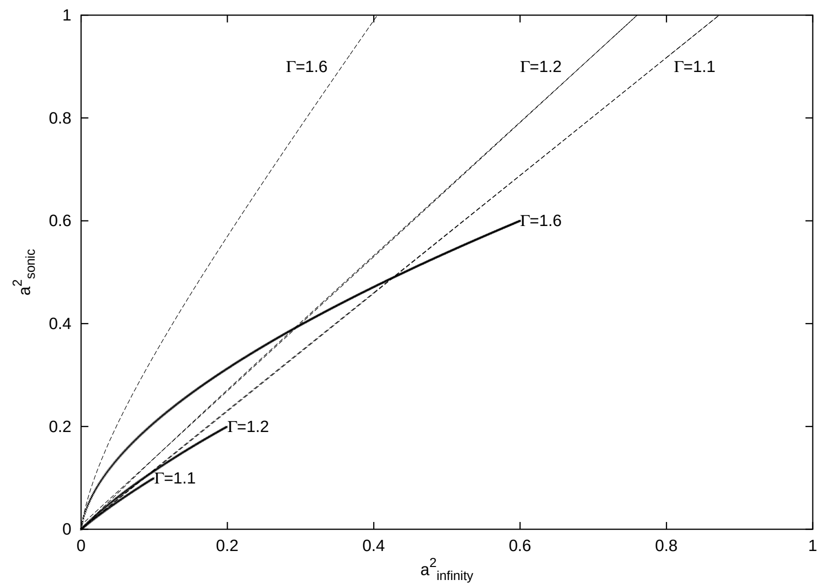

Fig. 1. Plot of a_s^2 in terms of a_∞^2 for three different values of the adiabatic index: $\Gamma=1.1$, $\Gamma=1.2$, and $\Gamma=1.6$. Solid and dotted curves refer to the $(\tilde{p}-n)$ model and the $(\tilde{p}-\varrho)$ model, respectively.

It should be mentioned that the equation (6) could be solved only by a numerical way while the parallel equation in the $(\tilde{p}-n)$ case (11) is analytically solved [7].

3.2. Fluid velocity

Fluid velocity as a function of a distance is described by Eqs. (12) and (7) for the $(\tilde{p}-n)$ model and the $(\tilde{p}-\varrho)$ model, respectively. It rises monotonically as the radius tends to the event horizon. Comparing both models we assume the same asymptotic sound velocity a_∞^2. As one can see (Figs. 2 and 3) both models predict similar values of u. We noticed that the greater Γ the slower fluid velocity at the given distance R.

Next conclusion is the confirmation of the fact (previously stated in [4]) that the value of u near the horizon strongly depends on the location of the sonic point $R_{\rm s}$. The further the sonic point the larger the fluid velocity and the closer to the speed of light at $R = 2M$.

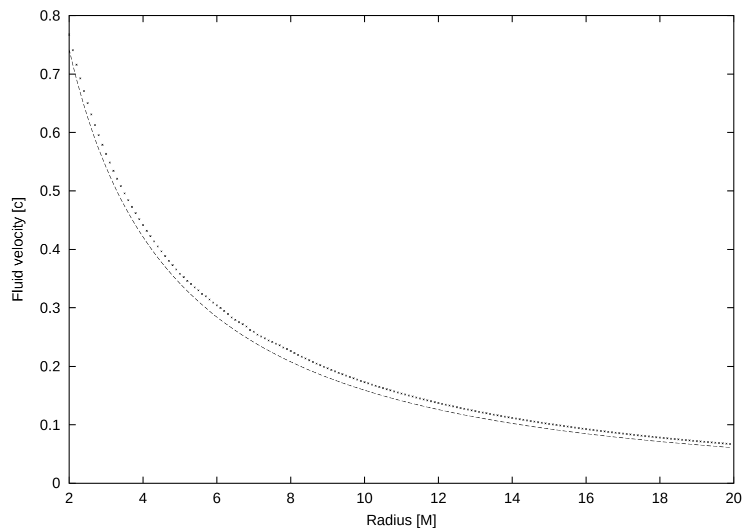

Fig. 2. Plot of fluid velocity u as a function of a radius R for $\Gamma = 1.1$ and $a_\infty^2 = 0.099$. Dotted and solid curves refer to the $(\tilde{p} - n)$ model and the $(\tilde{p} - \varrho)$ model, respectively.

3.3. Density profile

We recall here that the main difference between the $(\tilde{p} - n)$ model and the $(\tilde{p} - \varrho)$ model lies in the equations of state: $\tilde{p} = Cn^\Gamma$ and $\tilde{p} = K\varrho^\Gamma$, respectively. We can relate n and ϱ by

$$n = \exp\left(\int\limits_{\varrho_0}^{\varrho} d\varrho' \frac{1}{\varrho' + K\varrho'^\Gamma}\right) \tag{15}$$

that can be integrated with the result

$$n \cong \varrho\left(1 + K\varrho^{\Gamma-1}\right)^{1/(\Gamma-1)} = \varrho\left(1 + \frac{a^2}{\Gamma}\right)^{1/(\Gamma-1)} .$$

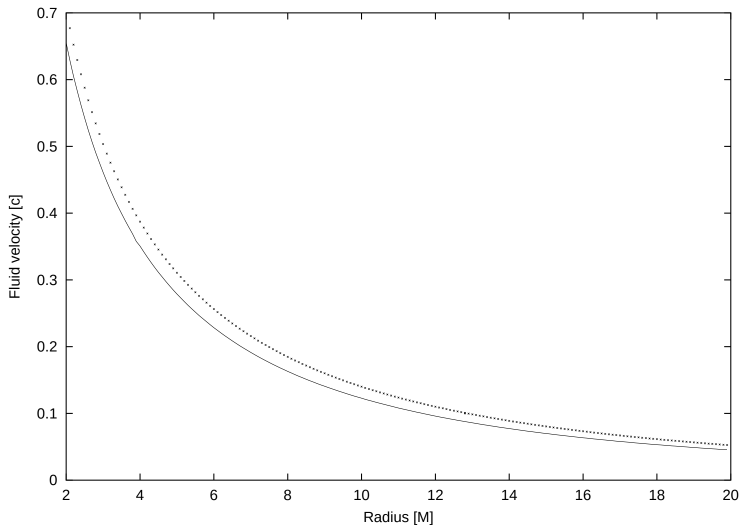

Fig. 3. Plot of fluid velocity u as a function of a radius R for $\Gamma = 1.4$ and $a_\infty^2 = 0.099$. Dotted and solid curves refer to the $(\tilde{p} - n)$ model and the $(\tilde{p} - \varrho)$ model, respectively.

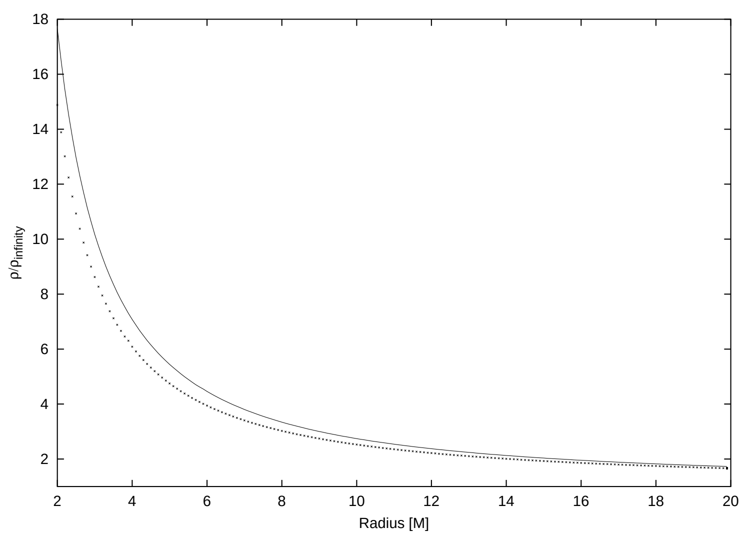

Fig. 4. Plot of nondimensional density profile ϱ/ϱ_∞ as a function of the distance R for the $(\tilde{p} - \varrho)$ model. The asymptotic velocity $a_\infty^2 = 0.099$ for both $\Gamma = 1.1$ (solid curve) and $\Gamma = 1.4$ (dotted curve).

Given the $(\tilde{p} - \varrho)$ polytropic model one can always find n. And conversely, one can find ϱ, given the polytropic $(\tilde{p}-n)$ model [6]. The preceding equation yields $n_\infty = \varrho_\infty$ if $a_\infty^2 \ll 1$; the same is true in the alternative description $(n - \tilde{p} \to \varrho)$ under the condition $\tilde{p}_\infty/(\Gamma - 1) \ll \varrho_\infty$ [6]. According to the numerical calculations when matter approaches the horizon its density increases (Figs. 4 and 5). We also noticed that the location of the sonic point R_s plays a very important role. If it is situated close to the horizon the density of matter there increases approximately to $10 \times \varrho_\infty$. On the other hand if $R_\mathrm{s} \gg 2M$ the density of matter approaching the horizon becomes few orders of magnitude greater than the asymptotic density. The predictions of the two models agree in the full spectrum of the values of index Γ.

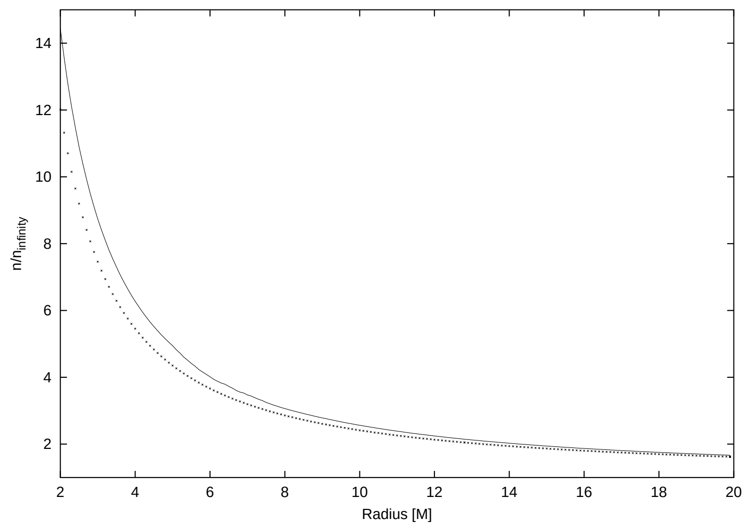

Fig. 5. Plot of nondimensional baryon density number profile n/n_∞ as a function of the distance R for the $(\tilde{p} - n)$ model. The asymptotic velocity $a_\infty^2 = 0.099$ for both $\Gamma = 1.1$ (solid curve) and $\Gamma = 1.4$ (dotted curve).

3.4. Mass accretion rate

In this subsection we compare the most important parameter to the description of accretion: mass accretion rate $\dot{M}$. For simplicity we introduce the parameter Ω which is defined as the ratio of mass accretion rate in relativistic model and the mass accretion rate predicted by the Bondi model: $\dot{M} = \Omega \dot{M}_\mathrm{B}$. Hence Ω can be interpreted as relativistic correction factor.

In the $(\tilde{p}-n)$ model this parameter, with help of (14), is expressed by

$$\Omega = a_\infty^3 \left(\frac{a_\mathrm{s}^2}{a_\infty^2} \sqrt{1+3a_\mathrm{s}^2} \right)^{1/(\Gamma-1)} \left(\frac{1+3a_\mathrm{s}^2}{a_\mathrm{s}^2} \right) \left(\frac{5-3\Gamma}{2} \right)^{(5-3\Gamma)/2(\Gamma-1)}, \quad (16)$$

while in the $(\tilde{p}-\varrho)$ model using (9) we get

$$\Omega = \left(\frac{(5-3\Gamma)a_\mathrm{s}^2}{2a_\infty^2} \right)^{\frac{5-3\Gamma}{2(\Gamma-1)}} \left(1+3a_\mathrm{s}^2\right) \left(1+\frac{a_s^2}{\Gamma}\right). \quad (17)$$

The comparison of the parameter Ω for the two models (Figs. 7 and 8) leads to the conclusion that they slightly differ in a full range of allowed a_∞^2, but it should be emphasized that the accretion in the $(\tilde{p}-n)$ model is more efficient.

Next we compare the relativistic correction factors as functions of the adiabatic index. We consider here an ultrarelativistic regime, *i.e.* we assume the maximum possible value of a_s^2. In [4] it was shown that for the $(\tilde{p}-\varrho)$ model the relativistic correction factor satisfies

$$4\left(1+\frac{1}{\Gamma}\right) \geq \Omega \geq 1.6\left(1+\frac{1}{\Gamma}\right). \quad (18)$$

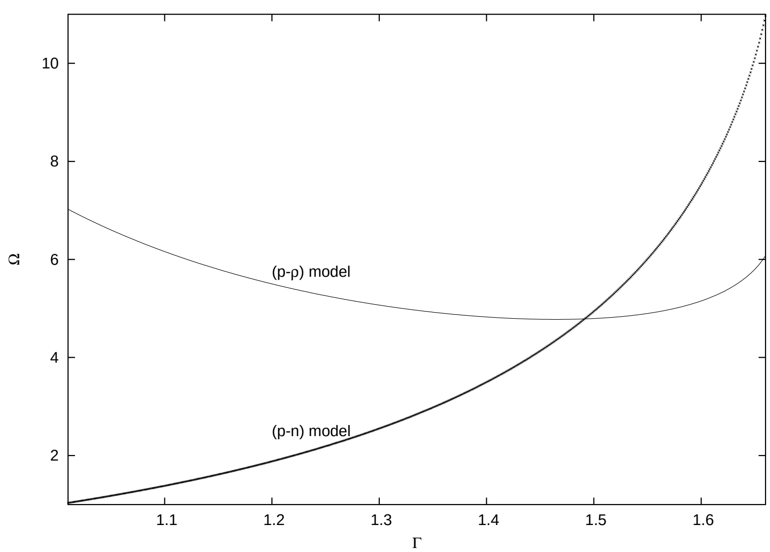

Fig. 6. Plot of the relativistic correction factor Ω as a function of the adiabatic index Γ for both models in ultrarelativistic regime. For each Γ the maximum possible a_s^2 is set.

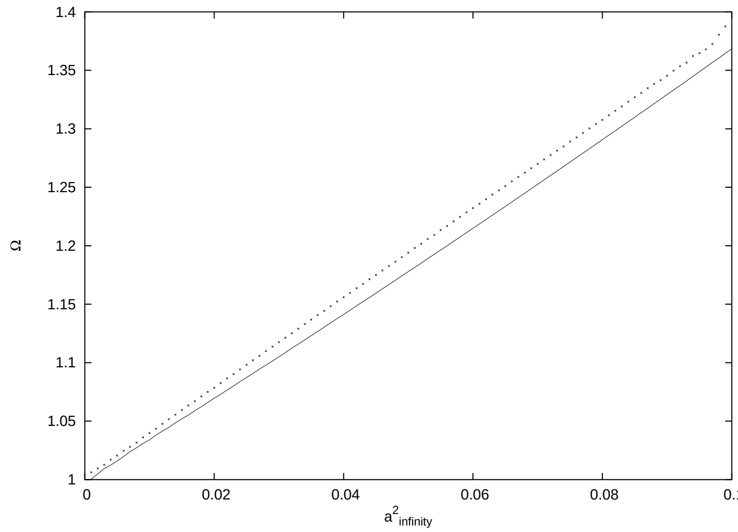

Fig. 7. Plot of the relativistic correction factor Ω as a function of asymptotic velocity of sound for fixed value of $\Gamma = 1.1$. Dotted and solid curves refers to the $(\tilde{p} - n)$ model and the $(\tilde{p} - \varrho)$ model, respectively.

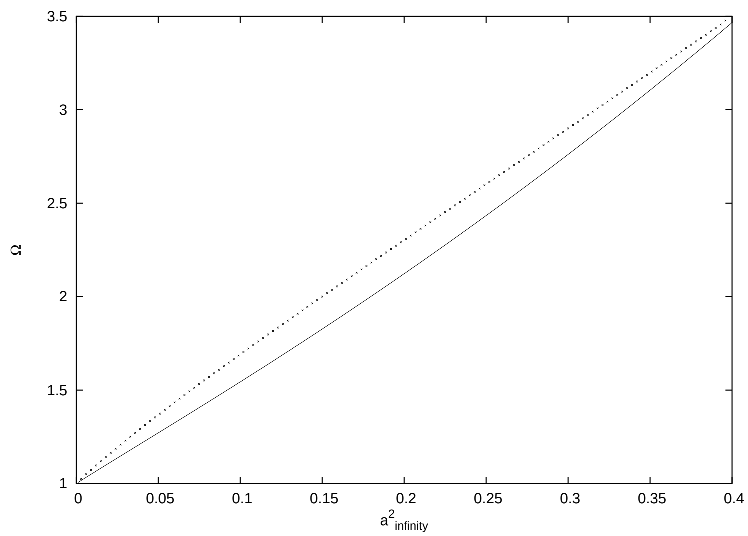

Fig. 8. Plot of the relativistic correction factor Ω as a function of asymptotic velocity of sound for fixed value of $\Gamma = 1.4$. Dotted and solid curves refer to the $(\tilde{p} - n)$ model and the $(\tilde{p} - \varrho)$ model, respectively.

We confirm here that the values of a parameter Ω belong to the range defined by (18). However, we revealed earlier [5] that the factor is not a monotonic function of Γ and for $\Gamma \approx 1.46$ it has a minimum of a value $\Omega \approx 4.77$. This is again confirmed by the present calculations. For the $(\tilde{p}-n)$ model Ω rises monotonically as Γ increases (Fig. 6).

It should be mentioned that in nonrelativistic case $a_{\mathrm{s}}^2 \ll 1$ the relativistic correction factor is close to 1 (Figs. 7 and 8), in full agreement with theoretical expectations [4].

4. Conclusions

We examined two models of stationary and spherically symmetrical accretion of gas onto a black hole. We show that both models essentially agree as it concerns quantities such as density profile and the mass accretion rate $\dot{M}$.

What drastically differentiate the models is the bound on the square of the sound velocity a^2. No such restriction appears in the $(\tilde{p}-\varrho)$ model. It makes this latter model more advantageous especially for the values of adiabatic index Γ close to 1 where the $(\tilde{p}-n)$ model provides the solutions only in a very narrow range of the asymptotic speed of sound. Another interesting difference can be observed in the ultrarelativistic regime and for Γ close to 1 and 5/3; the relativistic correction is significantly larger in the case of the $(\tilde{p}-n)$ model than in the $(\tilde{p}-\varrho)$ model.

The more general case of barotropic equations of state is being studied by Kinasiewicz *et al.* [7].

We wish to thank Professor Edward Malec for suggesting this topic of investigation and useful comments.

REFERENCES

[1] H. Bondi, *Mon. Not. R. Astron. Soc.* **112**, 192 (1952).

[2] F.C. Michel, *Astrophys. Space Sci.* **15**, 153 (1972).

[3] S. Shapiro, S. Teukolsky *Black Holes, White Dwarfs and Neutron Stars*, Wiley, New York 1983.

[4] E. Malec, *Phys. Rev.* **D60**, 104043 (1999).

[5] T. Lanczewski, M. Sc. Thesis, in Polish.

[6] J. Karkowski, E. Malec, *Class Quantum Grav.* **21**, 3923 (2004).

[7] B. Kinasiewicz, P. Mach, E. Malec, Z. Świerczyński, in preparation.